frontiers

Supplementary Material

1 TSUMAPS-NEAM: Extended project description

1.1 Project phases

Phase 1 (pre-assessment) was dedicated to selecting methods, data, and modeling alternatives, as well as to the first review. A hazard analysis is never completely constrained by observations, nor is the physics of the hazardous phenomenon totally understood. Different scientifically acceptable alternative models and relevant datasets may thus be used, thereby reflecting the inherent uncertainty. In Phase 1, after defining the basic methodology for the hazard analysis, the project development team (PDT) presented to the pool of experts (PE) a variety of possible alternative datasets and models, which could be used in the analysis. The PE guided the selection ("trimming") of these data and models in the first elicitation experiment by prioritizing the main uncertainty drivers. In other words, the implementation of a given input parameter or model was prioritized if the sensitivity of the hazard results to its variation or uncertainty was considered by the PE larger than the one from using another input. The team of internal reviewers (IR) then reviewed the resulting pre-assessment model. Most of the comments made by the IR were addressed and implemented in Phase 2, except for a few documented suggestions that resulted in being infeasible.

Phase 2 (assessment) concerned implementing the hazard workflow, including the weighting of the selected alternatives, building the final model, testing the results, and the second review round. The different alternative models may have different degrees of credibility within the reference scientific community. In principle, the model credibility should coincide with the accuracy of its output; but this is not always quantifiable because of the general lack of independent data for rare phenomena such as tsunamis. The second elicitation experiment with the PE established the relative weights of the selected alternative models. The PDT finalized the model accordingly, and the IR reviewed the NEAMTHM18 implementation and its results. The NEAMTHM18 results were then made available online for about one year to collect feedback from the broader community before its final release. The NEAMTHM18 was also presented in several scientific and professional contexts in search for the broadest possible feedback. The IR comments were included in the NEAMTHM18 Documentation and currently represent a guide for future versions of the NEAMTHM18.

Phase 3 (outreach) concerns the dissemination of results. Since the very beginning of the project, the preliminary, intermediate, and final results have been published on the project website. Phase 3 also includes the participation at scientific meetings and technical workshops for tsunami hazard prevention (e.g., IOC-UNESCO). Nowadays, it continues with scientific publications documenting general and specific components of the hazard model. The project website extensively illustrates project development and provide access to data. The making of NEAMTHM18 also involved producing several by-products that will be progressively distributed, depending on the availability of resources to finalize them. One example is the further development of relevant codes, such as the workflow based on high-performance computing (HPC) for site-specific high-resolution probabilistic tsunami hazard analysis (PTHA) (Gibbons et al., 2020) or the code for the computation of the earthquakes frequency-magnitude distribution (Taroni and Selva, 2020). All these elements guarantee that NEAMTHM18 remains persistently findable, accessible, interoperable, and reusable (FAIR).

1.2 By-products

The model by-products are represented by intermediate results of potential interest and relevance for other applications. The main output of Step-1 is a database of earthquake scenarios and relative mean annual rates. The source area covers all the Mediterranean, Marmara, and Black seas and a large area in the North Atlantic Ocean, including the Mid-Atlantic Ridge (north of the Equator) and the Caribbean Arc. At Step-2 we produced a database of pre-calculated tsunami scenarios for more than 120,000 elementary Gaussian sources (ca. 30 Tb of data) for an area of ca. 6x106 km^2 covering all the Mediterranean Sea, the Aegean Sea, the Marmara Sea, and the Black Sea, as well as a large area in the North Atlantic Ocean. This database allows for reproducing arbitrary tsunami scenarios using linear combinations of the Gaussian-shaped elementary sources distributed directly over the sea surface (Molinari et al., 2016). The main product of Step-3 is a database of local amplification factors based on the model proposed by Glimsdal et al. (2019). Amplification factors are evaluated for different incoming wave periods and polarities on the large set of local bathymetric profiles offshore target coastal areas. They can be applied to simulate the coastal impact (in terms of MIH) of any tsunami hitting the target area. Amplification factors have been evaluated for all the adopted POIs, covering the entire NEAM Region. Most of these products have already been used to produce short-term hazard quantifications for tsunami warning through the probabilistic tsunami forecasting method (Selva et al., 2019). To produce the main results described above, we put together a hazard calculation platform, which allows for the automatic quantification of the tsunami hazard model with alternative hazard models in the form of ensemble models. The model can be customized in terms of discretization, probabilistic models, propagation models, amplification models, and treatment of alternative implementations. The NEAMTHM18 Documentation (Basili et al., 2019) provides a more detailed description of these results and of the codes implemented in the hazard calculation platform.

1.3 Potential use-cases

A regional-scale model cannot replace in-depth analyses at sub-regional (national) and local levels, primarily because the regional-scale model resolution and spatial completeness are limited. The primary purpose of such a model, and consequently its usage, is that of a screening tool for prioritizing further higher-resolution hazard and risk assessments at a more local scale. Local models require very detailed calculations over coastal areas and high-resolution local data. Moreover, as mentioned above, an MIH of 1 m at some POI may indicate 3-4 m of maximum local run-up. The latter is yet another reason why a region-wide hazard assessment cannot replace detailed local hazard assessments. If the local scale is considered in any practical application based on the regional model, great caution is needed, and it must be understood that huge uncertainty would characterize this application. These uncertainties are necessarily larger than those stemming from a specific local high-resolution model. Nevertheless, a regional hazard assessment may provide informative input to decision-making like local studies under certain circumstances. The next section will describe a couple of such potential use-cases. However, these are just examples, and any further application reusing hazard data for risk-management applications and decision making is not necessarily straightforward.

Establishing a regional long-term PTHA for seismic sources is the first step for local and more detailed hazard analysis and subsequent risk assessment and management. Coastal planning, building codes definition, and safety of critical infrastructures all depend on these actions. The main advantage of the probabilistic approach in comparison with classical scenario-based methods is that it allows engineers to perform spatially homogeneous quantitative risk-analysis,

which allows decision-makers to base their choices on quantitative cost-benefit analyses and comparative studies between different areas, allowing for rational and ethical decisions.

1.3.1 From long-term hazard to evacuation maps for tsunami early warning

People can recognize an impending tsunami by warnings issued by a national authority or by observing natural signs, such as strong and unusually long shakings, receding seas, or roars from offshore. In both cases, it is crucial that people know in advance the possible escape routes toward higher and safer ground.

In the absence of a probabilistic tsunami hazard map, the local authorities usually follow expert advice coming from the scientific community. This can lead to the decision to set the limit of the tsunami hazard zone at a distance from the coast that corresponds to a certain topographic height or a maximum tsunami run-up. These distances may be spatially very inhomogeneous because they do not consider all possible scenarios, or because they may refer to scenarios with very different Average return Periods (ARPs). Using probabilistic tsunami hazard maps can help to make these decisions less subjective. The inundation distance corresponding to a design Probability of Exceedance (PoE) or ARP, potentially considering uncertainty for increasing safety, can be extrapolated with approximated methods from the MIH provided by NEAMTHM18. For example, one can consider the relationship between MIH and maximum run-up and various approaches to consider wave energy dissipation on large inundation distances. This type of approach is being followed in New Zealand (MCDEM, 2016). The Italian Civil Protection Department has also followed this approach for establishing the national guidelines for local planning against tsunamis (DCDPC, 2018).

1.3.2 Setting priorities for local probabilistic inundation maps in hazard and risk analyses

Local hazard analyses can be expensive and time-consuming and should then be standardized and prioritized, for instance, starting with the most hazardous areas. Standardization can be based on the comparison with a common regional analysis. A prioritization based on the selection of an ARP suitable for a specific application (e.g., an ARP of 2,475 years is being proposed for building codes by civil engineers in the USA) can ease the work of decision-makers (Wood et al., 2020). The priority assessment can be done by comparing the regional-scale hazard at different locations for that specific ARP. Other aspects to take into consideration are the locally exposed coastal population or the infrastructures, thus basing the prioritization also on elements at risk (Løvholt et al., 2015; Triantafyllou et al., 2019; Argyroudis et al., 2020; Wood et al., 2020).

Local tsunami hazard analysis requires the use of state-of-the-art high-performance computing, provided that high-resolution digital elevation models are available for nearshore and onshore areas. To limit the computational cost, the analysts may need to select a limited number of high-resolution inundation scenarios (Lorito et al., 2015; Volpe et al., 2019), for which regional hazards may provide the first screening. The relevant scenarios for a given site under examination can be selected using NEAMTHM18 results, from where detailed simulations could be performed without compromising the results of the analysis.

Supplementary Table 1. Results of elicitation #1. Ranking of the alternatives in all Steps and Levels. Color legend: High priority, Medium priority, Low priority. PS: Predominant Seismicity; BS: Background Seismicity. Concerning the implementation of Steps, alternatives are strongly encouraged for Step-1 and Step-3 only. The potential influence of alternatives in Step-4 should be tested. Alternatives can be avoided in Step-2. Within Step-1, alternatives are strongly encouraged to select the subduction interfaces to be separately modeled, and the quantification of the frequency/magnitude distribution. Alternatives are recommended for the seismic catalogs to consider, and the location and slip distribution models on subduction interfaces. Within Step-2 (if alternatives were to be considered), alternatives are strongly encouraged for the topo-bathymetric datasets and digital elevation models. Alternatives are recommended for coseismic displacement models, tsunami generation models, and tsunami propagation (in deepwater) models. Within Step-3, alternatives are strongly encouraged for topo-bathymetric datasets and digital elevation models, for amplification and inundation models at the points of interest (POIs), and onshore, corresponding to the offshore points of Step-2, and for models of the uncertainty on the tsunami metrics. Within Step-4, alternatives are recommended for the quantifications of weights by the experts and weights of alternative models.

Prioritization of Steps

No.	Model code	Description
1	Step-1	Definition of the seismic source variability and quantification of the long-run frequencies of all the seismic sources
2	Step-2	Tsunami generation and offshore propagation
3	Step-3	Near-shore tsunami propagation and inundation
4	Step-4	Computation of the weights of the alternative models developed in Steps 1 to 3 to measure their credibility, and construction of the “ensemble” model

Prioritization of Levels in Step-1

No.	Model code	Description
1	Region	Level-0 - Regionalization
2	PSDef	Level-0 - Selection of interfaces to be modeled separately
3	SeismicCat	Level-0 - Seismic catalogues
4	FreqMag	Level-1 - Quantification of the Magnitude-frequency (of PS and BS, separately)
5	PS-Pos	Level-2a - Sublevel PS-1: spatial distribution (position and area) and average slip of earthquakes over PS
6	PS-Slip	Level-2a - Sublevel PS-2: slip distribution of PS
7	BS-Pos	Level-2b - Sublevel BS-1/2: hypocenter distribution of BS
8	BS-Mech	Level-2b - Sublevel BS-3: focal mechanism of BS
9	BS-Size	Level-2b - Sublevel BS-4: size of finite faults of BS (scaling relations)
10	BS-Slip	Level-2b - Sublevel BS-5: slip distribution of BS

Prioritization of Levels in Step-2

No.	Model code	Description
1	Crust	Level-0 - Crustal models (elastic parameters)
2	TopoBath	Level-0 - Topo-bathymetric datasets and digital elevation models
3	CoSeis	Level-1 - Coseismic displacement model
4	TsuGen	Level-2 - Tsunami generation model
5	TsuProp	Level-3 - Tsunami propagation (in deep water) model

Prioritization of Levels in Step-3

No.	Model code	Description
1	TopoBath	Level-0 - Topo-bathymetric datasets and digital elevation models
2	Inund	Level-1 - Amplification and inundation models at the points of interest along the coast, and inland, corresponding to the offshore points of Step-2
3	Tide	Level-2 – Evaluation of the probability of tidal stage at the points of interest
4	Uncertainty	Level-3 - Model the uncertainty on the tsunami metrics

Prioritization of Levels in Step-4

No.	Model code	Description
1	WeightsExperts	Level-0 – Quantification of weights of the experts
2	Aggregation	Level-1 – Method for aggregating hazard results within each model
3	WeightsModels	Level-2 – Quantification of the weights of alternative models
4	EpisIntegration	Level-2 – Method for integrating the alternative models into a single model that quantifies also the epistemic uncertainty (e.g., Logic Tree, Ensemble models)

Supplementary Table 2. Results of elicitation #2. Weights assigned to the implemented alternative models.

Step/Level - Question	Alternative models	Ensemble weight
Step-1 – Level-0 Question 1	Cut-off distance of 5 km around the PS sources	0.39
	Cut-off distance of 10 km around the PS sources	0.61
Step-1 – Level-1 Question 2a	Mean annual rates for PS and BS jointly quantified	0.44
	Mean annual rates for PS and BS independently quantified	0.56
Step-1 – Level-1 Question 2b	Tapered FMD (with probability > 0 for all magnitudes) with the parameter β set to 2/3 (equivalent to b-value = 1), independently from data.	0.30
	Tapered FMD (with probability > 0 for all magnitudes) with the parameter β set from data.	0.31
	Truncated FMD (with probability = 0 for all $M > M_{max}$) with the parameter β set from data.	0.19
	Truncated FMD (with probability = 0 for all $M > M_{max}$) with the parameter β set to 2/3 (equivalent to b-value = 1), independently from data.	0.20
Step-1 – Level-2 Question 3a	Scaling relations from Strasser et al. (2010).	0.55
	Scaling relations from Murotani et al. (2013).	0.45
Step-1 – Level-2 Question 3b	Co-seismic slip is not allowed or allowed to occur at shallow depths under the accretionary wedge.	0.34
	Co-seismic slip can happen at shallow depths under the accretionary wedge.	0.66
Step-1 – Level-2 Question 3c	Rigidity is uniform with depth (PREM).	0.35
	Rigidity varies with depth according to Geist and BiIek (2001).	0.65
Step-4 – Level-0 Question 4	Performance-based weights (PB)	0.57
	Acknowledgement-based weights (AB)	0.43
Step-4 – Level-0 Question 0	Criterion 1: Expert's personal preference	0.64
	Criterion 2: Most used in the community according to the expert's best knowledge	0.36

Supplementary Table 3. Year of completeness for the macro-regions and the relevant earthquake catalog. The value "-1" corresponds to a completeness year not assigned.

Macro-region	Catalog	M 3.5	M 4.0	M 4.5	M 5.0	M 5.5	M 6.0	M 6.5	M 7.0	M 7.5	M 8.0
Iceland	ISC	1996	1996	1980	1980	1972	1972	1944	1944	1944	1944
Caribbean	ISC	2000	2000	1970	1970	1965	1965	1902	1902	1902	1902
NE Atlantic	ISC	1996	1996	1965	1965	1952	1952	1944	1944	1944	1944
W Mediterranean	EMEC	-1	2000	1970	1950	1910	1750	1350	1350	1350	1350
Circum-Adriatic	EMEC	-1	2000	1960	1920	1905	1850	1450	1450	1450	1450
NW Europe	EMEC	2000	1980	1960	1900	1880	1550	1550	1550	1550	1550
Black Sea & Caucasus	EMEC	-1	-1	1950	1920	1900	1850	1550	1550	1550	1550
Aegean - Anatolia - Arabia	EMEC	-1	2000	1965	1911	1905	1750	1550	1100	1050	1050
W Africa	ISC	2009	2009	1975	1975	1940	1940	1940	1940	1940	1940
N Africa	EMEC	-1	-1	1960	1930	1910	1890	1850	1700	1700	1700

Supplementary Table 4. Parameters for the frequency-magnitude distribution to be derived from tectonic data based on Christophersen et al. (2015) and Davies et al. (2018).

	Calabrian Arc	Hellenic Arc	Cyprus Arc	Caribbean Arc	Gloria Fault	Gibraltar Arc
Convergence or slip rate (mm/y)	1.75	10.00	6.77	11.00	4.00	3.96
Coupling 1	0.30	0.20	0.30	0.30	0.30	0.30
Coupling 2	0.50	0.60	0.50	0.50	0.50	0.50
Coupling 3	0.70	1.00	0.70	0.70	0.70	0.70
b-value 1	0.70	0.70	0.70	0.70	0.70	0.70
b-value 2	0.95	0.95	0.95	0.95	0.95	0.95
b-value 3	1.20	1.20	1.20	1.20	1.20	1.20
Mmax 1	7.60	8.00	7.70	8.00	8.30	8.20
Mmax 2	8.10	8.60	8.30	8.80	8.60	8.40
Mmax 3	9.00	9.10	9.00	9.60	8.80	8.60

Supplementary Table 5. Magnitude discretization. The third column shows the magnitude values for which tsunami scenarios are numerically modeled for each interval. These values are set as the mean seismic moment of the interval bounds defined in the first two columns, computed assuming a standard Gutenberg-Richter distribution with a b-value equal to 1. The intervals are used for determining earthquake rates.

#	Interval lower end	Interval upper end	Interval mean	Increment
1	5.700	6.338	6.000	
2	6.338	6.672	6.500	0.500
3	6.672	6.937	6.801	0.301
4	6.937	7.218	7.074	0.273
5	7.218	7.427	7.320	0.247
6	7.427	7.666	7.544	0.223
7	7.666	7.827	7.745	0.202
8	7.827	8.033	7.928	0.183
9	8.033	8.155	8.093	0.165
10	8.155	8.334	8.243	0.150
11	8.334	8.423	8.378	0.135
12	8.423	8.580	8.501	0.123
13	8.580	8.643	8.612	0.111
14	8.643	8.783	8.712	0.100
15	8.783	8.823	8.803	0.091
16	8.823	8.948	8.885	0.082
17	8.948	8.970	8.959	0.074
18	8.970	9.084	9.026	0.067

Supplementary Table 6. Parameters of subfaults in the Mid-Atlantic Ridge zone (including Gloria fault). Parameters from scaling relations are: Mw=moment magnitude; M_0=seismic moment; L=fault length; W=fault width; A=fault area; D=slip. L*, A*, D* are approximated length, area, and slip obtained by combining one or more subfaults; ΔA and ΔD are the deviations from the theoretical values for area and slip, respectively.

A) Normal faults (spreading ridges): fixed patch size: L = 40, W = 45; total number of patches = 214

M_w	M_0 (Nm)	L (km)	W (km)	A (km^2)	D (m)	N. subfaults	L* (km)	A* (km)	ΔA (km^2)	D* (m)	ΔD (m)
7.320	1.22E+20	70	30	2091	1.94	1	40	1800	-291	2.25	0.31
7.544	2.63E+20	96	37	3495	2.51	2	80	3600	105	2.44	-0.07
7.745	5.28E+20	127	44	5563	3.17	3	120	5400	-163	3.26	0.10
7.928	9.93E+20	163	52	8472	3.91	5	200	9000	528	3.68	-0.23

B) Strike-slip faults (transforms): fixed patch size: L=55, W=20; total number of patches=56

M_w	M_0 (Nm)	L (km)	W (km)	A (km^2)	D (m)	N. subfaults	L* (km)	A* (km)	ΔA (km^2)	D* (m)	ΔD (m)
7.320	1.22E+20	112	19	2139	1.90	2	110	2200	61	1.84	-0.05
7.544	2.63E+20	188	19	3577	2.45	3	165	3300	-277	2.66	0.21
7.745	5.28E+20	299	19	5692	3.09	5	275	5500	-192	3.20	0.11
7.928	9.93E+20	455	19	8670	3.82	8	440	8800	130	3.76	-0.06
8.093	1.76E+21	666	19	12685	4.20	12	660	13200	515	4.04	-0.16
8.243	2.95E+21	940	19	17902	4.99	16.	880	17600	-302	5.07	0.09

Supplementary Table 7. Ranges of earthquake magnitude and seismogenic depth for Mediterranean subduction interfaces modeled as Predominant Seismicity (PS) type.

	Calabrian Arc (PS)	Hellenic Arc (PS)	Cyprus Arc (PS)
Minimum magnitude	6	6	6
Maximum Magnitude w/ very shallow seismicity not allowed + Strasser et al. (2010) scaling relation	8.1	8.9	8.5
Maximum Magnitude w/ very shallow seismicity not allowed + Murotani et al. (2013) scaling relation	8.1	8.7	8.4
Seismogenic depth interval (km from the mean sea level) w/ very shallow seismicity not allowed	44-15.5	56.5-14	48.5-5.5
Maximum Magnitude w/ very shallow seismicity allowed + Strasser et al. (2010) scaling relation	8.6	9	8.5
Maximum Magnitude w/ very shallow seismicity allowed + Murotani et al. (2013) scaling relation	8.6	9	8.4
Seismogenic depth interval (km from the mean sea level) w/ very shallow seismicity allowed	44-6.8	56.5-8.8	48.5-5.5

Supplementary Table 8. Ranges of earthquake magnitude and seismogenic depth for Atlantic subduction interfaces and crustal faults modeled as Predominant Seismicity (PS), Special PS (SPS), and Special Background Seismicity (SBS) types.

	Caribbean Arc (PS)	Strike-Slip Mid-Atlantic Ridge and Gloria Fault (SPS)	Dip-Slip Mid-Atlantic Ridge (SPS)	Strike-Slip Distant Mid-Atlantic Ridge (PS)	Dip-Slip Distant Mid-Atlantic Ridge (PS)	Gibraltar Arc (SBS)
Minimum magnitude	7.3	6	6	7.3	7.3	6
Maximum magnitude	9	8.2	7.9	8.2	7.9	9
Seismogenic depth interval (km from the seafloor)	48-1	20-0	37-0	20-0	37-0	75-0

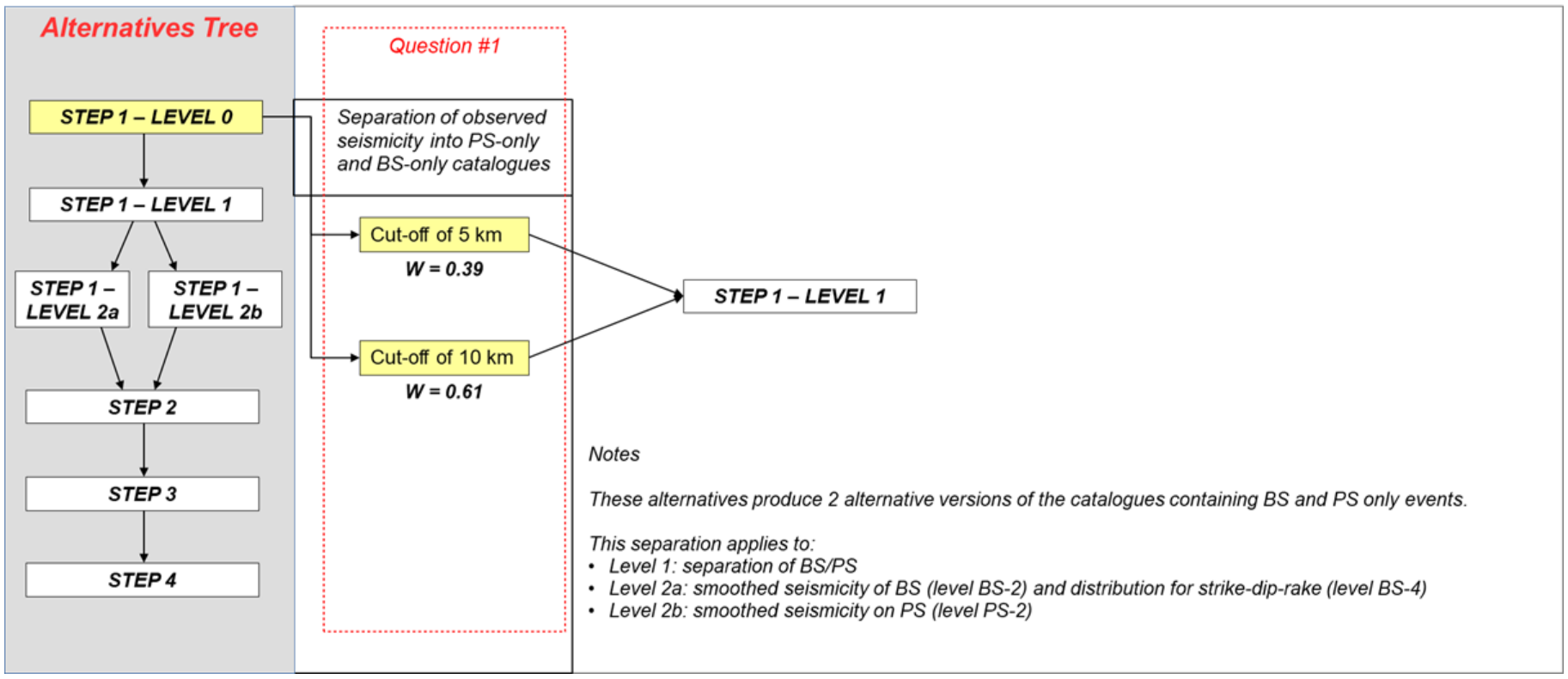

Supplementary Figure 1. Implementation of model alternatives in all Steps and Levels (continues in the next two pages) as the outcome of the two elicitation experiments reported in **Supplementary Table 1 and Supplementary Table 2**. The last panel shows (third page) the Event Tree scheme detailing STEP 1 for BS and PS. A common magnitude discretization is applied at Level 1 to both PS and BS annual rates. See also the definition of Steps and Levels and the description of the elicitation experiments in the main text.

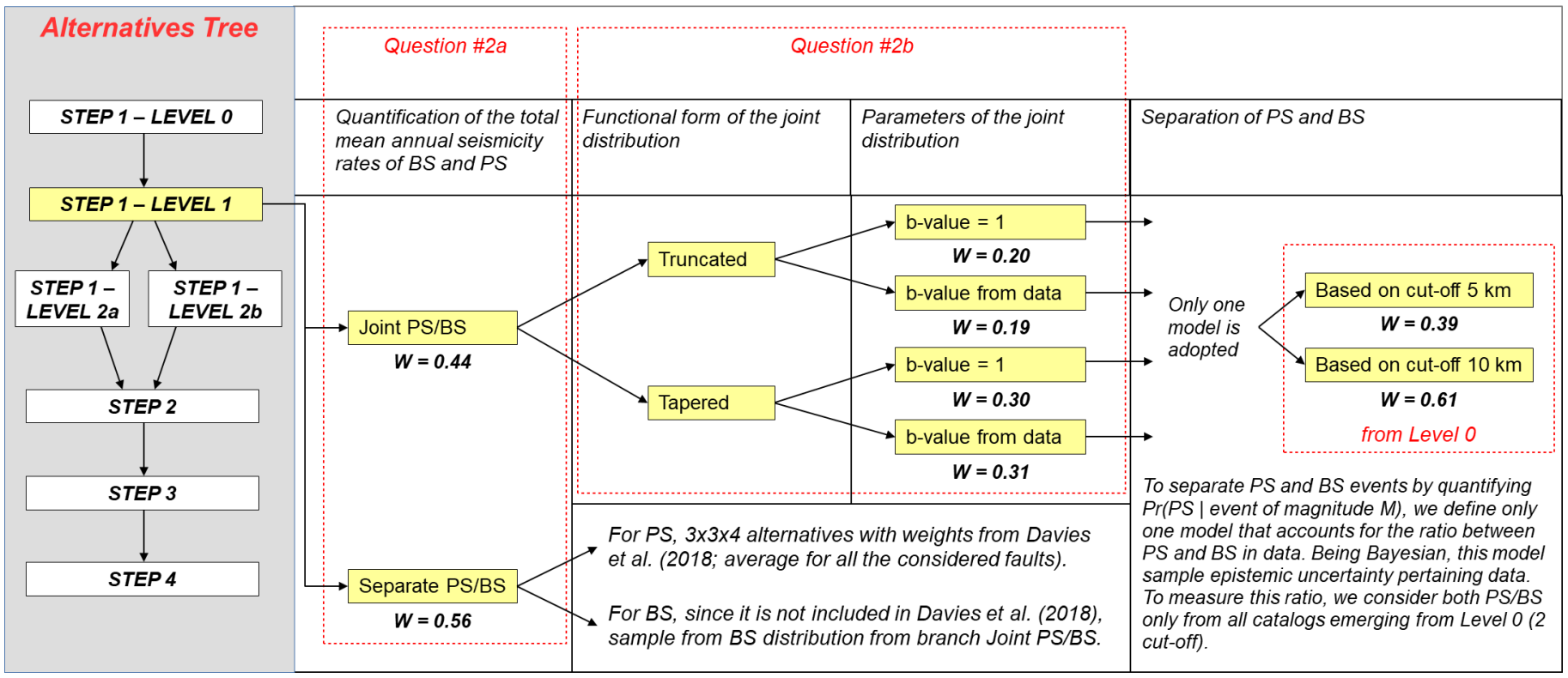
Alternatives Tree
STEP 1 – LEVEL 0
STEP 1 – LEVEL 1
STEP 1 – LEVEL 2a
STEP 1 – LEVEL 2b
STEP 2
STEP 3
STEP 4
Question #2a
Question #2b
Quantification of the total mean annual seismicity rates of BS and PS
Functional form of the joint distribution
Parameters of the joint distribution
Separation of PS and BS
Joint PS/BS
W = 0.44
Separate PS/BS
W = 0.56
Truncated
Tapered
b-value = 1
W = 0.20
b-value from data
W = 0.19
b-value = 1
W = 0.30
b-value from data
W = 0.31
For PS, 3x3x4 alternatives with weights from Davies et al. (2018; average for all the considered faults).
For BS, since it is not included in Davies et al. (2018), sample from BS distribution from branch Joint PS/BS.
Only one model is adopted
Based on cut-off 5 km
W = 0.39
Based on cut-off 10 km
W = 0.61
from Level 0
To separate PS and BS events by quantifying Pr(PS | event of magnitude M), we define only one model that accounts for the ratio between PS and BS in data. Being Bayesian, this model sample epistemic uncertainty pertaining data. To measure this ratio, we consider both PS/BS only from all catalogs emerging from Level 0 (2 cut-off).

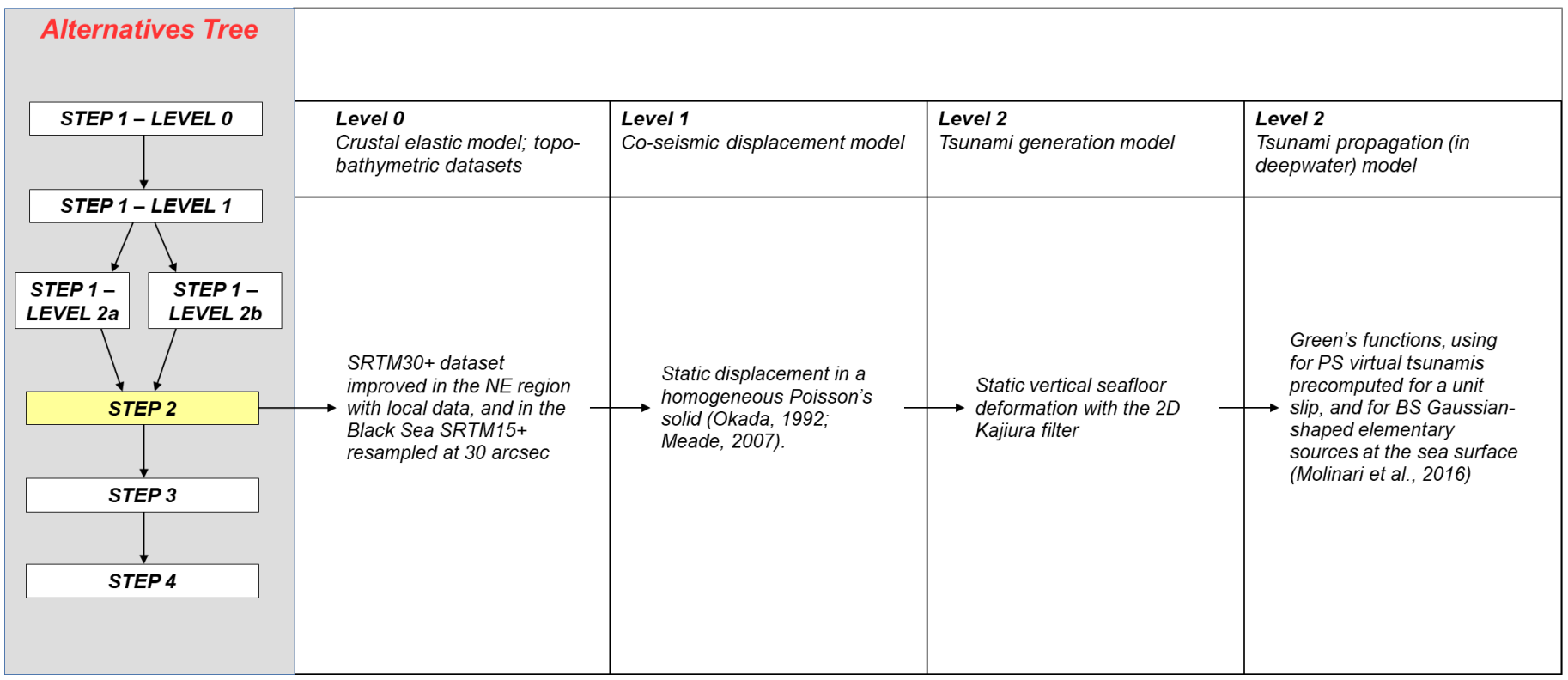
Alternatives Tree
STEP 1 – LEVEL 0
STEP 1 – LEVEL 1
STEP 1 – LEVEL 2a
STEP 1 – LEVEL 2b
STEP 2
STEP 3
STEP 4
Level 0
Crustal elastic model; topo-bathymetric datasets
Level 1
Co-seismic displacement model
Level 2
Tsunami generation model
Level 2
Tsunami propagation (in deepwater) model
SRTM30+ dataset improved in the NE region with local data, and in the Black Sea SRTM15+ resampled at 30 arcsec
Static displacement in a homogeneous Poisson's solid (Okada, 1992; Meade, 2007).
Static vertical seafloor deformation with the 2D Kajiura filter
Green's functions, using for PS virtual tsunamis precomputed for a unit slip, and for BS Gaussian-shaped elementary sources at the sea surface (Molinari et al., 2016)

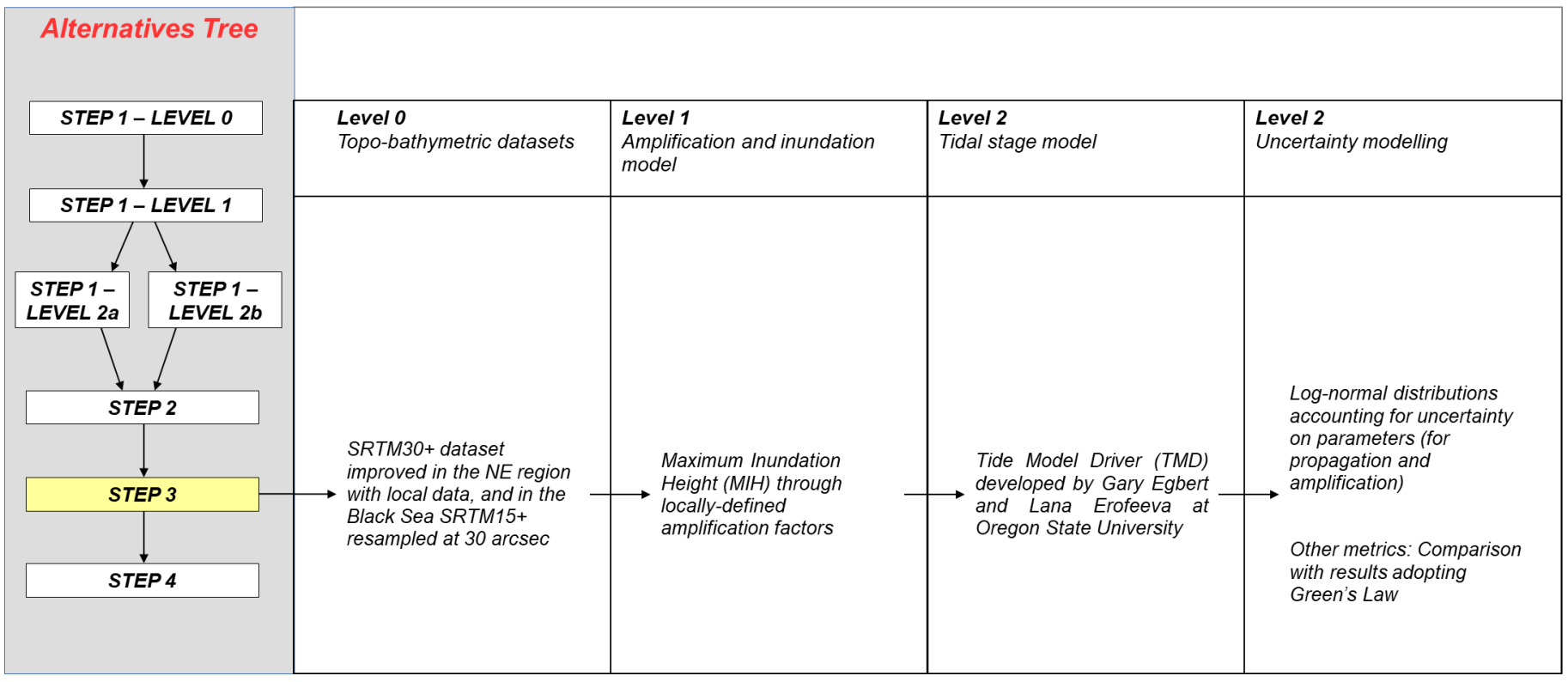
Alternatives Tree
STEP 1 – LEVEL 0
STEP 1 – LEVEL 1
STEP 1 – LEVEL 2a
STEP 1 – LEVEL 2b
STEP 2
STEP 3
STEP 4
Level 0
Topo-bathymetric datasets
Level 1
Amplification and inundation model
Level 2
Tidal stage model
Level 2
Uncertainty modelling
SRTM30+ dataset improved in the NE region with local data, and in the Black Sea SRTM15+ resampled at 30 arcsec
Maximum Inundation Height (MIH) through locally-defined amplification factors
Tide Model Driver (TMD) developed by Gary Egbert and Lana Erofeeva at Oregon State University
Log-normal distributions accounting for uncertainty on parameters (for propagation and amplification)
Other metrics: Comparison with results adopting Green's Law

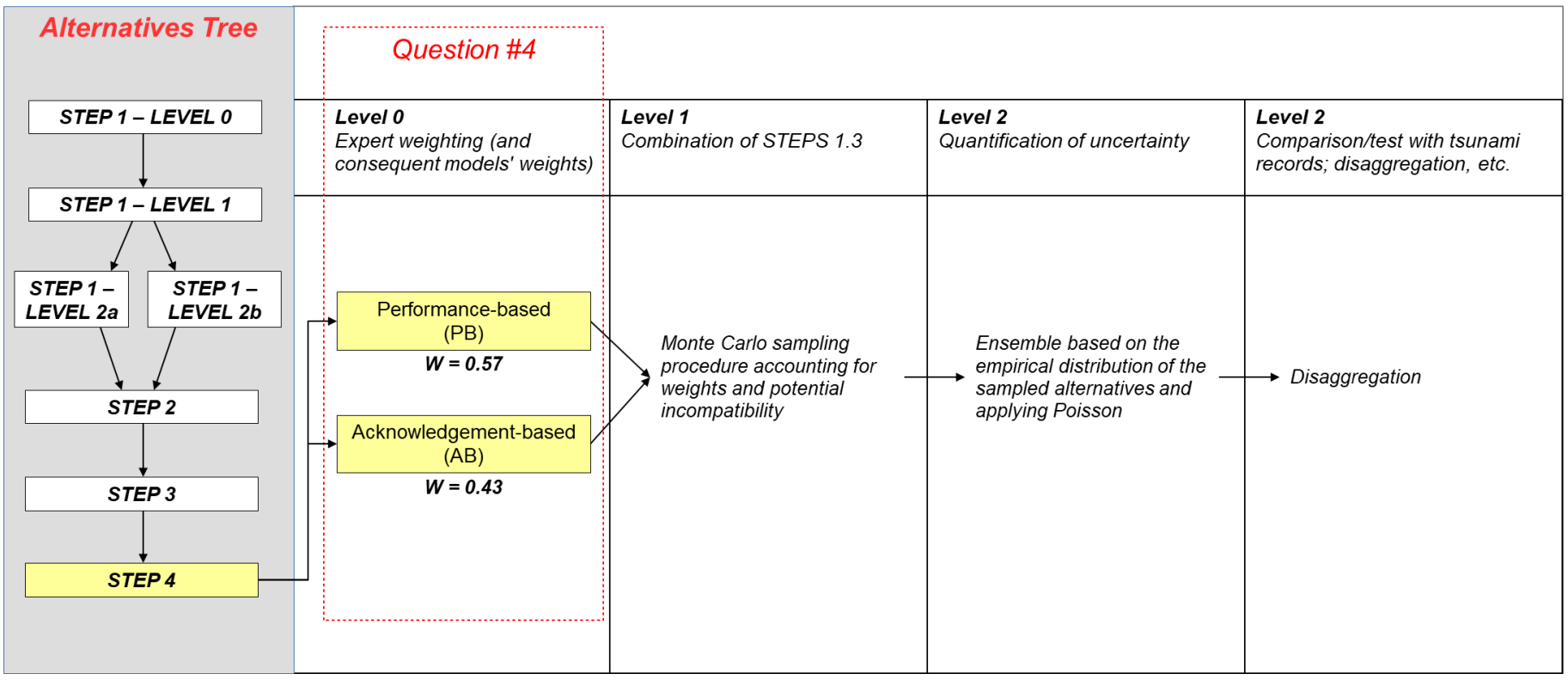
Alternatives Tree
Question #4
STEP 1 – LEVEL 0
STEP 1 – LEVEL 1
STEP 1 – LEVEL 2a
STEP 1 – LEVEL 2b
STEP 2
STEP 3
STEP 4
Level 0
Expert weighting (and consequent models' weights)
Level 1
Combination of STEPS 1.3
Level 2
Quantification of uncertainty
Level 2
Comparison/test with tsunami records; disaggregation, etc.
Performance-based (PB)
W = 0.57
Acknowledgement-based (AB)
W = 0.43
Monte Carlo sampling procedure accounting for weights and potential incompatibility
Ensemble based on the empirical distribution of the sampled alternatives and applying Poisson
Disaggregation

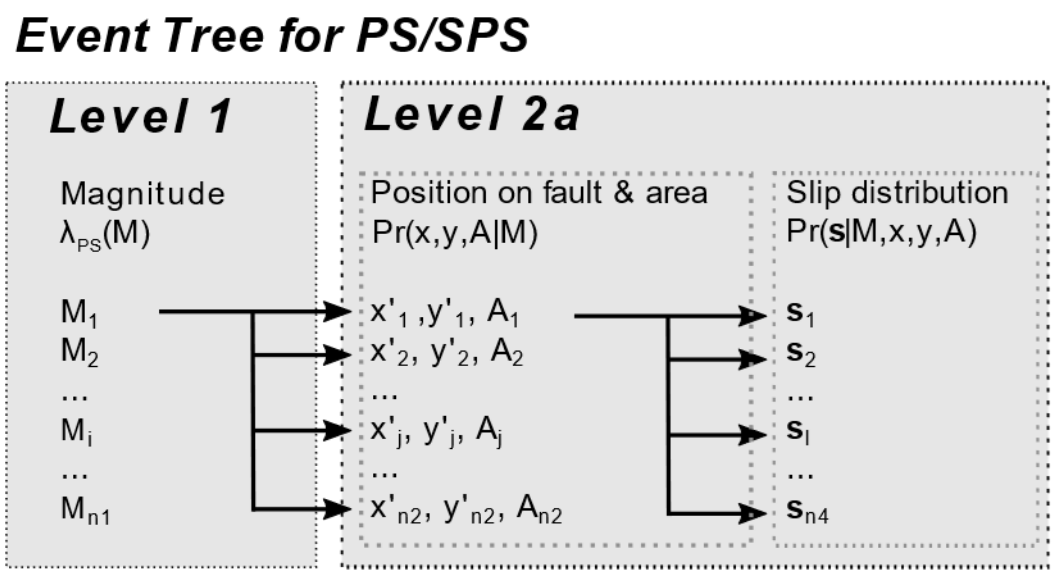
Event Tree for PS/SPS
Level 1
Magnitude
λPS(M)
M1
M2
...
Mi
...
Mn1
Level 2a
Position on fault & area
Pr(x,y,A|M)
x'1 ,y'1, A1
x'2, y'2, A2
...
x'j, y'j, Aj
...
x'n2, y'n2, An2
Slip distribution
Pr(s|M,x,y,A)
s1
s2
...
sl
...
sn4

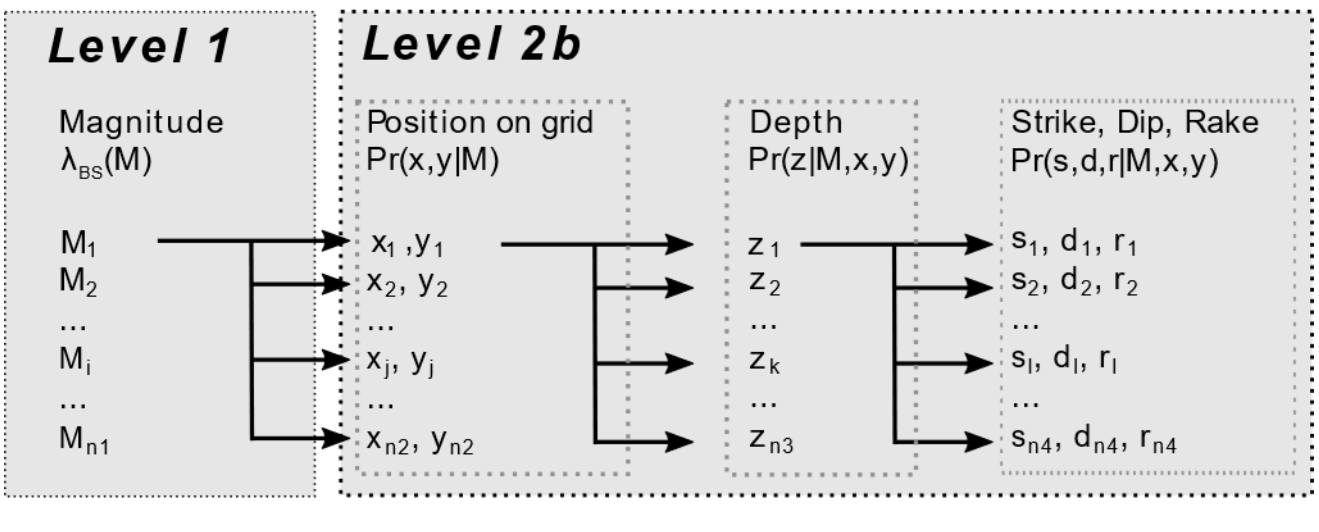
Event Tree for BS/SBS
Level 1
Magnitude
λBS(M)
M1
M2
...
Mi
...
Mn1
Level 2b
Position on grid
Pr(x,y|M)
x1 ,y1
x2, y2
...
xj, yj
...
xn2, yn2
Depth
Pr(z|M,x,y)
z1
z2
...
zk
...
zn3
Strike, Dip, Rake
Pr(s,d,r|M,x,y)
s1, d1, r1
s2, d2, r2
...
sl, dl, rl
...
sn4, dn4, rn4

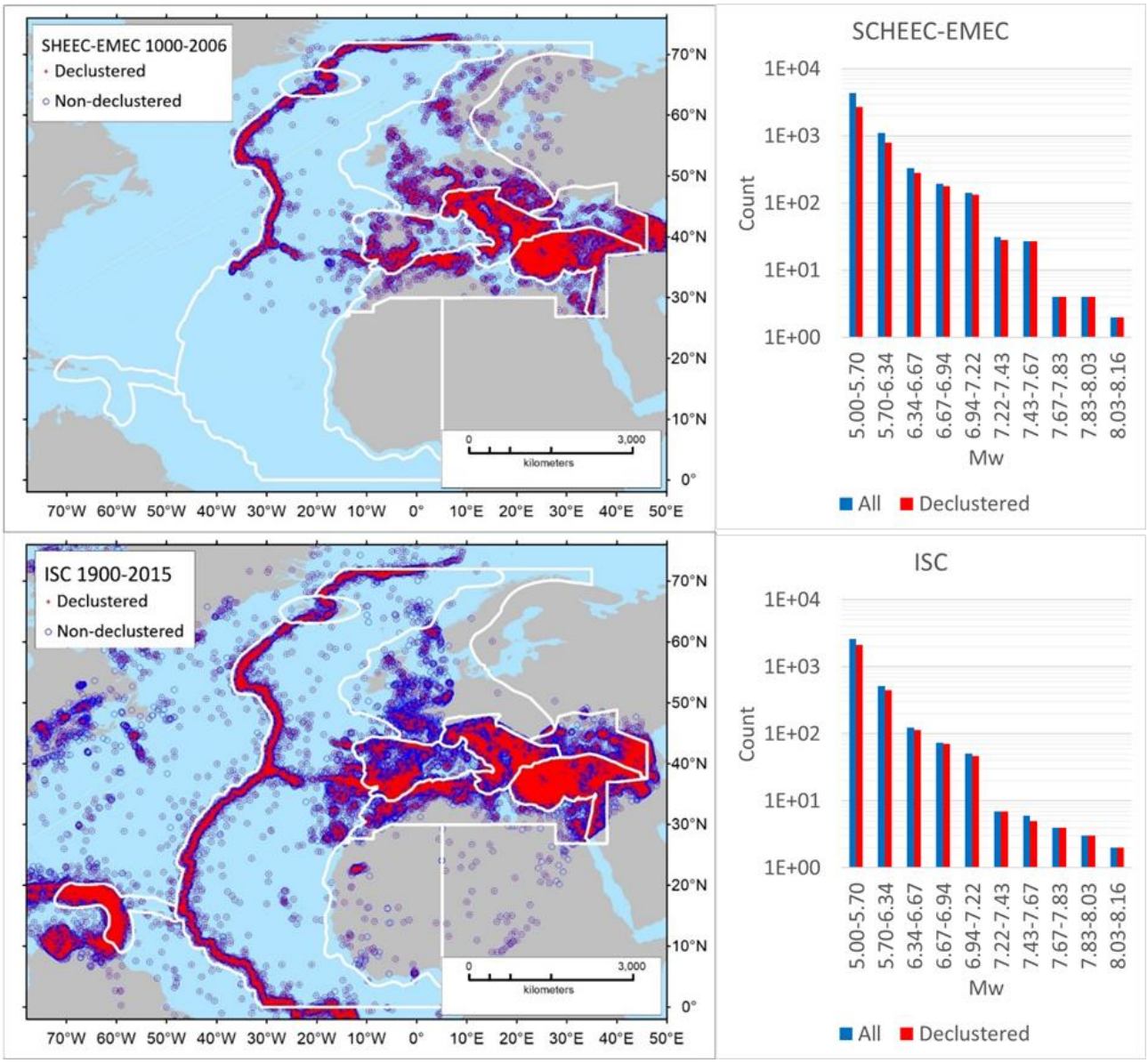

Supplementary Figure 2. Geographic and frequency-magnitude distributions of the SHEEC-EMEC and ISC earthquake catalogs (Grünthal and Wahlström, 2012; Stucchi et al., 2013; ISC, 2016) for both the declustered and non-declustered versions. The regions of **Figure 4B** in the main text are shown with a white outline for reference. The histogram classes correspond to intervals in **Supplementary Table 5**.

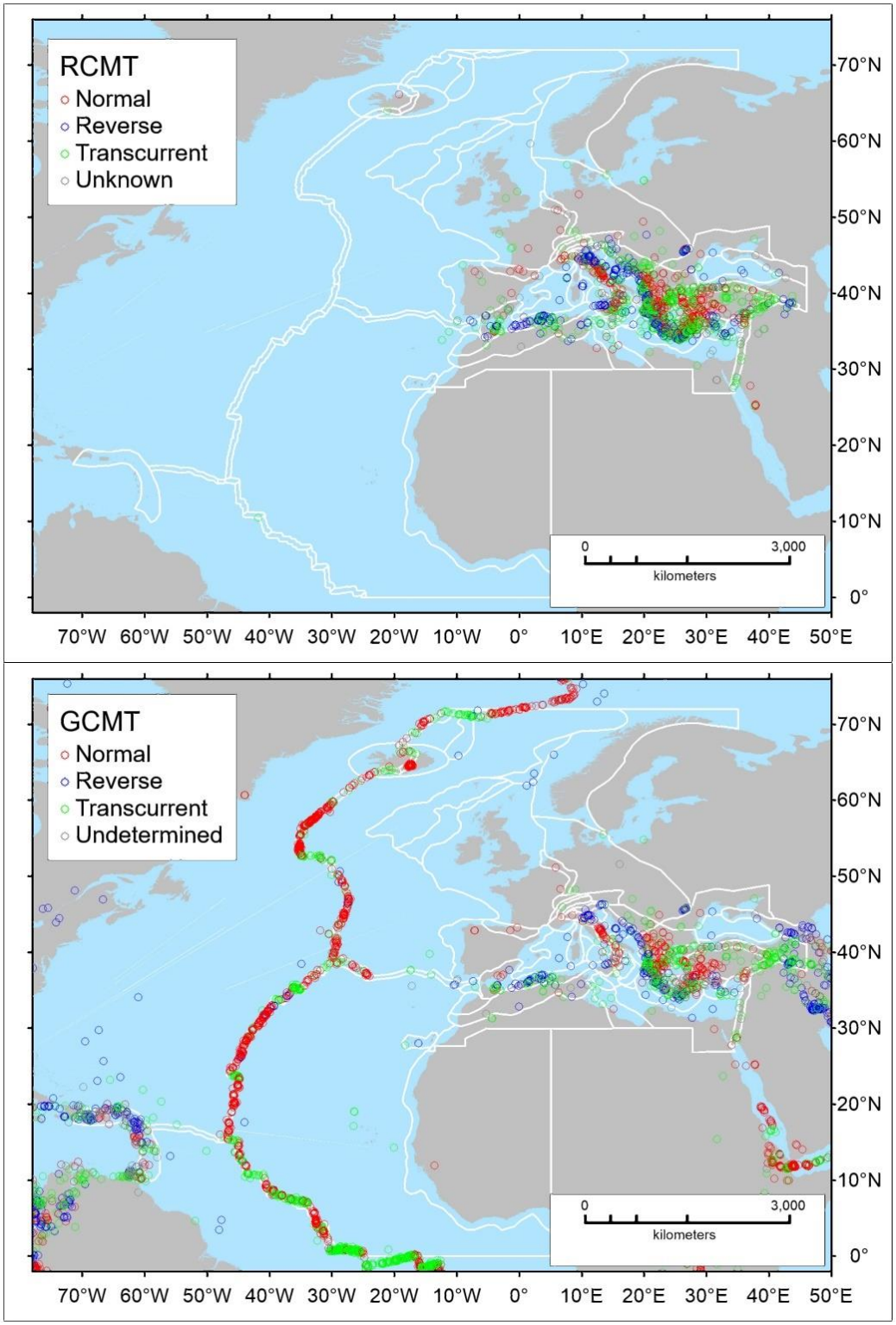

Supplementary Figure 3. Geographic distribution of the catalogs of focal mechanisms, color-coded based on their mechanism. GCMT: Global Centroid Moment Tensors (Dziewonski et al., 1981; Ekström et al., 2012), RCMT: Regional Centroid Moment Tensors (Pondrelli and Salimbeni, 2015). The tectonic regions of **Figure 4A** are shown with a white outline for reference.

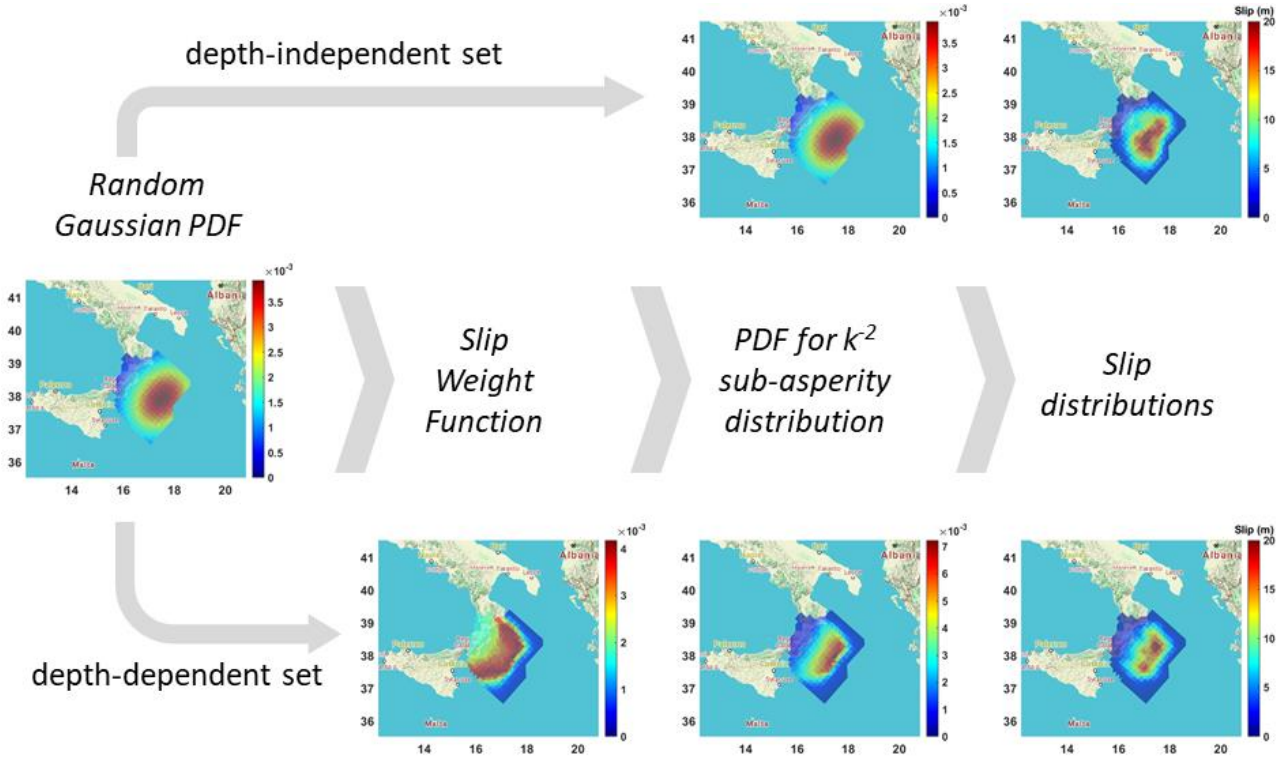

Supplementary Figure 4. Sketch of the two workflows for the definition of the slip distributions from Scala et al. (2020). Two slip distribution sets are developed. One is obtained by combining a random Gaussian PDF with a slip weight function based on the depth-dependent rigidity and relative coupling, to define a depth-dependent PDF controlling the location of slip over the 3D mesh. The other is obtained by letting the random Gaussian PDF coincide with the PDF for k^{-2} slip distribution and then combining it with homogeneous rigidity and relative coupling. Further implications on these distributions have been discussed by Davies (2019) and Davies and Griffin (2020).

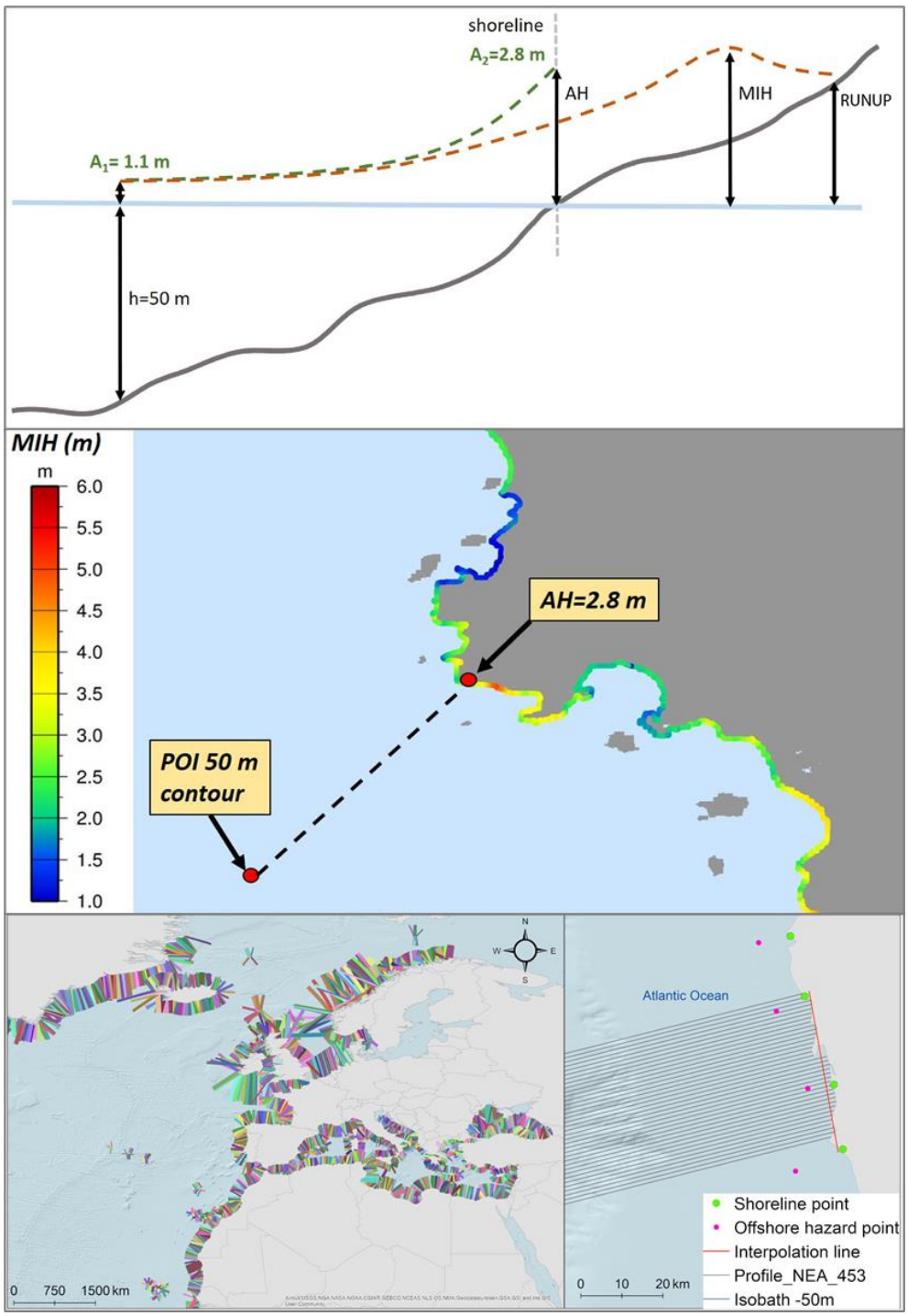

Supplementary Figure 5. (Top) Schematic representation of Maximum Inundation Height (MIH) and its estimator, the Amplified Height AH, was obtained with the amplification factors. More details in the text. (Middle) Sketch of the lateral MIH variability behind a given Point of Interest (POI). (Bottom left) Map of transects for the analysis of the amplification factors covering the entire NEAM Region and (Bottom right) detail of a sample transect showing the correspondence between POIs, transects, and onshore hazard points. Figure modified after Glimsdal et al. (2019).

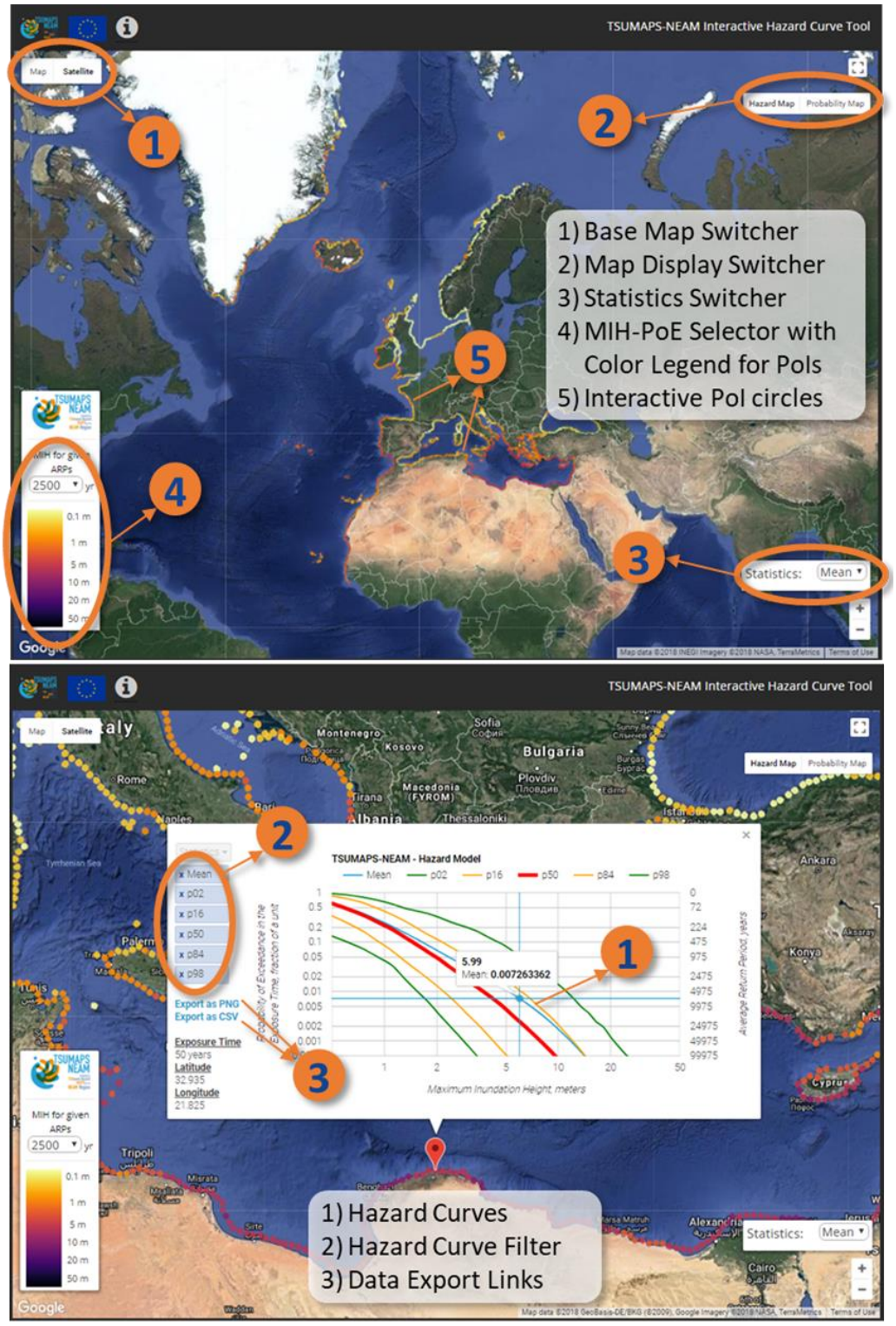

Supplementary Figure 6. Screenshots of the interactive tool (http://www.tsumaps-neam.eu/neamthm18/). Map display tools (top) and curve display tools (bottom).

References

Argyroudis, S. A., Fotopoulou, S., Karafagka, S., Pitilakis, K., Selva, J., Salzano, E., et al. (2020). A risk-based multi-level stress test methodology: application to six critical non-nuclear infrastructures in Europe. *Nat. Hazards* 100, 595–633. doi:10.1007/s11069-019-03828-5.

Basili, R., Brizuela, B., Herrero, A., Iqbal, S., Lorito, S., Maesano, F. E., et al. (2019). NEAMTHM18 Documentation: the making of the TSUMAPS-NEAM Tsunami Hazard Model 2018. *Ist. Naz. Geofis. E Vulcanol. INGV*, 352. doi:10.5281/zenodo.3406625.

Christophersen, A., Berryman, K., and Litchfield, N. (2015). The GEM Faulted Earth Project, Version 1.0. *GEM Faulted Earth Proj.* April 2015. doi:10.13117/GEM.GEGD.TR2015.02.

Davies, G. (2019). Tsunami variability from uncalibrated stochastic earthquake models: tests against deep ocean observations 2006–2016. *Geophys. J. Int.* 218, 1939–1960. doi:10.1093/gji/ggz260.

Davies, G., and Griffin, J. (2020). Sensitivity of Probabilistic Tsunami Hazard Assessment to Far-Field Earthquake Slip Complexity and Rigidity Depth-Dependence: Case Study of Australia. *Pure Appl. Geophys.* doi:10.1007/s00024-019-02299-w.

Davies, G., Griffin, J., Løvholt, F., Glimsdal, S., Harbitz, C., Thio, H. K., et al. (2018). A global probabilistic tsunami hazard assessment from earthquake sources. *Geol. Soc. Lond. Spec. Publ.* 456, 219–244. doi:10.1144/sp456.5.

DCDPC (2018). Indicazioni alla Componenti ed alle Strutture operative del Servizio nazionale di protezione civile per l'aggiornamento delle pianificazioni di protezione civile per il rischio maremoto. Presidenza del Consiglio dei Ministri – Dipartimento della Protezione Civile.

Dziewonski, A. M., Chou, T.-A., and Woodhouse, J. H. (1981). Determination of earthquake source parameters from waveform data for studies of global and regional seismicity. *J. Geophys. Res. Solid Earth* 86, 2825–2852. doi:10.1029/JB086iB04p02825.

Ekström, G., Nettles, M., and Dziewoński, A. M. (2012). The global CMT project 2004–2010: Centroid-moment tensors for 13,017 earthquakes. *Phys. Earth Planet. Inter.* 200–201, 1–9. doi:10.1016/j.pepi.2012.04.002.

Gibbons, S. J., Lorito, S., Macías, J., Løvholt, F., Selva, J., Volpe, M., et al. (2020). Probabilistic Tsunami Hazard Analysis: High Performance Computing for Massive Scale Inundation Simulations. *Front. Earth Sci.* doi:Under review.

Glimsdal, S., Løvholt, F., Harbitz, C. B., Romano, F., Lorito, S., Orefice, S., et al. (2019). A New Approximate Method for Quantifying Tsunami Maximum Inundation Height Probability. *Pure Appl. Geophys.* 176, 3227–3246. doi:10.1007/s00024-019-02091-w.

Grünthal, G., and Wahlström, R. (2012). The European-Mediterranean Earthquake Catalogue (EMEC) for the last millennium. *J. Seismol.* 16, 535–570. doi:10.1007/s10950-012-9302-y.

ISC (2016). *On-line Bulletin*. International Seismological Centre Available at: http://www.isc.ac.uk.

Lorito, S., Selva, J., Basili, R., Romano, F., Tiberti, M. M., and Piatanesi, A. (2015). Probabilistic hazard for seismically induced tsunamis: accuracy and feasibility of inundation maps. *Geophys. J. Int.* 200, 574–588. doi:10.1093/gji/ggu408.

Løvholt, F., Griffin, J., and Salgado-Gálvez, M. A. (2015). "Tsunami Hazard and Risk Assessment on the Global Scale," in *Encyclopedia of Complexity and Systems Science*, ed. R. A. Meyers (Berlin, Heidelberg: Springer Berlin Heidelberg), 1–34. doi:10.1007/978-3-642-27737-5_642-1.

MCDEM (2016). *Tsunami Evacuation Zones - Director's Guideline for Civil Defence Emergency Management Groups*. New Zealand: Ministry of Civil Defence & Emergency Management Available at: https://www.civildefence.govt.nz/assets/Uploads/publications/dgl-08-16-Tsunami-Evacuation-Zones.pdf.

Molinari, I., Tonini, R., Lorito, S., Piatanesi, A., Romano, F., Melini, D., et al. (2016). Fast evaluation of tsunami scenarios: uncertainty assessment for a Mediterranean Sea database. *Nat. Hazards Earth Syst. Sci.* 16, 2593–2602. doi:10.5194/nhess-16-2593-2016.

Murotani, S., Satake, K., and Fujii, Y. (2013). Scaling relations of seismic moment, rupture area, average slip, and asperity size for *M* ~9 subduction-zone earthquakes. *Geophys. Res. Lett.* 40, 5070–5074. doi:10.1002/grl.50976.

Pondrelli, S., and Salimbeni, S. (2015). "Regional Moment Tensor Review: An Example from the European–Mediterranean Region," in *Encyclopedia of Earthquake Engineering*, eds. M. Beer, I. A. Kougioumtzoglou, E. Patelli, and I. S.-K. Au (Berlin, Heidelberg: Springer Berlin Heidelberg), 1–15. doi:10.1007/978-3-642-36197-5_301-1.

Scala, A., Lorito, S., Romano, F., Murphy, S., Selva, J., Basili, R., et al. (2020). Effect of Shallow Slip Amplification Uncertainty on Probabilistic Tsunami Hazard Analysis in Subduction Zones: Use of Long-Term Balanced Stochastic Slip Models. *Pure Appl. Geophys.* 177, 1497–1520. doi:10.1007/s00024-019-02260-x.

Selva, J., Lorito, S., Perfetti, P., Tonini, R., Romano, F., Bernardi, F., et al. (2019). Probabilistic Tsunami Forecasting (PTF) for Tsunami Early Warning operations. in *Geophysical Research Abstracts* (Vienna, Austria), EGU2019-17775. Available at: https://meetingorganizer.copernicus.org/EGU2019/EGU2019-17775.pdf [Accessed September 26, 2020].

Strasser, F. O., Arango, M. C., and Bommer, J. J. (2010). Scaling of the Source Dimensions of Interface and Intraslab Subduction-zone Earthquakes with Moment Magnitude. *Seismol. Res. Lett.* 81, 941–950. doi:10.1785/gssrl.81.6.941.

Stucchi, M., Rovida, A., Gomez Capera, A. A., Alexandre, P., Camelbeeck, T., Demircioglu, M. B., et al. (2013). The SHARE European Earthquake Catalogue (SHEEC) 1000–1899. *J. Seismol.* 17, 523–544. doi:10.1007/s10950-012-9335-2.

Taroni, M., and Selva, J. (2020). GR_EST: an OCTAVE/MATLAB toolbox to estimate Gutenberg-Richter law parameters and their uncertainties. *Seismol. Res. Lett.* in press.

Triantafyllou, I., Novikova, T., Charalampakis, M., Fokaefs, A., and Papadopoulos, G. A. (2019). Quantitative Tsunami Risk Assessment in Terms of Building Replacement Cost Based on

Tsunami Modelling and GIS Methods: The Case of Crete Isl., Hellenic Arc. *Pure Appl. Geophys.* 176, 3207–3225. doi:10.1007/s00024-018-1984-9.

Volpe, M., Lorito, S., Selva, J., Tonini, R., Romano, F., and Brizuela, B. (2019). From regional to local SPTHA: efficient computation of probabilistic tsunami inundation maps addressing near-field sources. *Nat. Hazards Earth Syst. Sci.* 19, 455–469. doi:10.5194/nhess-19-455-2019.

Wood, N., Peters, J., Wilson, R., Sherba, J., and Henry, K. (2020). Variations in community evacuation potential related to average return periods in probabilistic tsunami hazard analysis. *Int. J. Disaster Risk Reduct.*, 101871. doi:10.1016/j.ijdrr.2020.101871.